

Electronic Supplementary Information

A highly specific 'Turn-On' fluorescent detection of Mg^{2+} through a xanthene based fluorescent molecular probe

Abha Pandey, Ajit Kumar, Siddharth Vishwakarma, K. K. Upadhyay*

Department of Chemistry (Centre of Advanced Study), Faculty of Science, Banaras Hindu University, Varanasi, Uttar Pradesh-221005, India.

*Corresponding author: Tel: +91 542 670 2488

E-mail: drkaushalbhu@yahoo.co.in; kku@bhu.ac.in, Tel: +91-542-6702488

Table of Contents

S No.	Figures	Captions	Page No.
1.		Experimental section	3
2.	Table S1	Crystal data and structure refinement for B-XAN	4-5
3.	Figure S1	IR spectrum of B-XAN	6
4.	Figure S2	1H NMR spectrum of B-XAN (in CD_3CN)	7
5.	Figure S3	^{13}C NMR spectrum of B-XAN (in $DMSO-d_6$)	8
6.	Figure S4	ESI-MS spectrum of B-XAN	9
7.	Figure S5	IR spectrum of N-XAN	10
8.	Figure S6	1H NMR spectrum of N-XAN (in $DMSO-d_6$)	11
9.	Figure S7	^{13}C NMR spectrum of N-XAN (in $DMSO-d_6$)	12
10.	Figure S8	ESI-MS spectrum of N-XAN	13
11.	Figure S9	IR spectrum of $(B-XAN)_2Mg$	14
12.	Figure S10	1H NMR spectrum of $(B-XAN)_2Mg$ (in CD_3CN)	15
13.	Figure S11	^{13}C NMR spectrum of $(B-XAN)_2Mg$ (in $DMSO-d_6$)	16

Electronic Supplementary Information

14.	Figure S12	ESI-MS spectrum of (B-XAN) ₂ Mg	17
15.	Figure S13(a)	UV-visible Spectrum of B-XAN in presence of different metal ions (10 equiv.) at 10 μM in acetonitrile	18
16.	Figure S13(b)	Photograph showing naked eye color change of B-XAN (under visible light) in presence of different metal ions in acetonitrile	18
17.	Figure S14(a)	UV-visible Spectrum of N-XAN with different metal ions (10 equiv.) at 10 μM in acetonitrile	19
18.	Figure S14(b)	Photograph showing naked eye colour change of N-XAN (under visible light) in presence of different metal ions in acetonitrile	19
19.	Figure S15(a)	Relative fluorescence changes of N-XAN (1.0 μM) after addition of 10 equiv. of various metal ions in acetonitrile at 458 nm along with inset fluorescence spectral graph	20
20.	Figure S15(b)	Naked eye fluorescence response of N-XAN in the presence of different metal ions (under UV light of 365 nm)	20
21.	Figure S16	Fluorescence responses of B-XAN (1μM) at 458 nm in the presence of various metal ions in acetonitrile solution. The red bars represent the emission intensities of B-XAN in the presence of various metal ions (10.0 eq.). The blue bars represent the change of emission upon subsequent addition of Mg ²⁺ (10.0 eq.) to the above solutions	21
22.	Figure S17	Calibration curve for determination of detection limit of B-XAN for Mg ²⁺ by fluorescence titration data	22
23.	Figure S18	Job's Plot between B-XAN and Mg ²⁺ showing 2:1 binding stoichiometry	23
24.	Figure S19	Reaction-time profile of B-XAN in presence of Mg ²⁺	24
25.	Figure S20	Fluorescence emission spectra showing reversibility of B-XAN in the presence of Mg ²⁺ and EDTA in acetonitrile solution	25
26.	Figure S21	Non-linear fit plot of fluorescence titration data for determination of binding constants.	26

Electronic Supplementary Information

EXPERIMENTAL SECTION

Instrumentation:

The IR Spectra for the **B-XAN**, **N-XAN** and **(B-XAN)₂Mg** were recorded on JASCO-FTIR Spectrophotometer while ¹H NMR spectra were recorded on JEOL AL 300 FT NMR Spectrometer Mass spectrometric analysis was carried out on a Bruker Compass data analysis spectrometer. Electronic spectra were recorded at room temperature (298 K) on a UV-1800 pharماسpec spectrophotometer with quartz cuvette (path length=1 cm). Emission spectra were recorded on Varian Cary Eclipse Fluorescence spectrophotometer and JY HORIBA Fluorescence spectrophotometer. The ¹H NMR spectra were recorded by using tetramethylsilane (TMS) as an internal reference standard.

Materials and methods:

All reagents for synthesis were purchased from Sigma-Aldrich and were used without any further purification. All titration experiments were carried at room temperature. All the cations were used as their chloride salts. The ¹H NMR spectra were recorded by using tetramethylsilane (TMS) as an internal reference standard.

X-ray crystallographic studies:

Single crystal X-ray diffraction measurements were carried out on an Oxford Diffraction Xcalibur system with a Ruby CCD detector. All the determinations of unit cell and intensity data were performed with graphite-mono-chromated Mo-K α radiation ($\lambda = 0.71073 \text{ \AA}$). Data for the ligand and metal complex were collected at room temperature. The structures were solved by direct methods, using Fourier techniques, and refined by full-matrix least-squares on F2 using the SHELXTL-97 program package [1]. Crystal data and details of the structure determination for ligand and complex are summarized in Table 1. **CCDC 1059288** contains the supplementary crystallographic data for this paper. These data can be obtained free of charge from the Cambridge Crystallographic Data Centre via <http://www.ccdc.cam.ac.uk/cgi-bin/catreq.cgi>.

References:

1. (a) G. M. Sheldrick, SHELXL-97, Program for X-ray Crystal Structure Refinement, Göttingen University, Göttingen, Germany, 1997; (b) G. M. Sheldrick, SHELXS-97, Program for X-ray Crystal Structure Solution, Göttingen University, Göttingen, Germany, 1997.

Electronic Supplementary Information

Table 1: Crystal data and details of the structure determination of **B-XAN**:

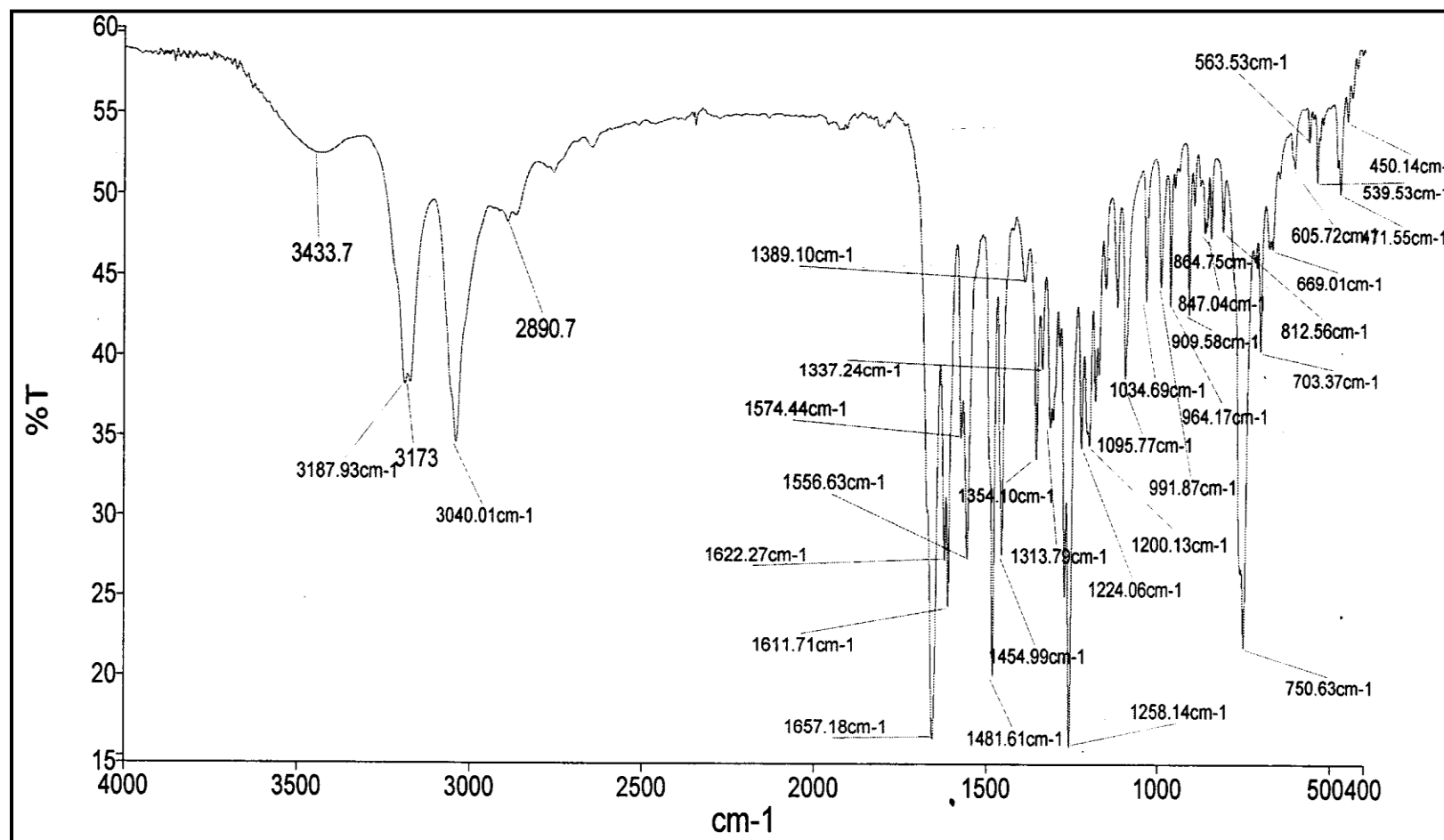
Identification code	B-XAN
CCDC No.	CCDC 1059288
Empirical formula	C ₂₁ H ₁₆ N ₂ O ₃
Formula weight	344.36
Temperature	293(2) K
Wavelength	0.71073Å
Crystal system	Monoclinic
space group	P21/c
Unit cell dimensions	a=16.7245(10)Å , alpha=90deg. b=11.3341(6) Å, beta=105.028(5) deg. c=9.6962(5) Å, gamma=90deg.
Volume	1775.12(17) Å ³
Z	4
Density (calculated)	1.288 mg/m ³
Absorption coefficient	0.087 mm ⁻¹
F(000)	720.0
Crystal size	0.028 x 0.023 x 0.016 mm
Crystal color and habit	Colourless, needle
Diffractionmeter	'Xcalibur, Eos'
Theta range for data collection	3.31 to 29.16 deg.
Limiting indices	-22<=h<=22, -9<=k<=15, -12<=l<=13
Reflections collected / unique	8177 / 4800 [R(int) = 0.0196]
Completeness to theta = 25.00	99.8 %
Absorption correction	Semi-empirical from equivalents
Refinement method	Full-matrix least-squares on F ²
Max. and min. transmission	1.00000 and 0.93478
Data / restraints / parameters	4034 / 0 / 236

Electronic Supplementary Information

Goodness-of-fit on F^2	1.053
Final R indices [$I > 2\sigma(I)$]	R1 = 0.0515, wR2 = 0.1104
R indices (all data)	R1 = 0.0856, wR2 = 0.1321
Largest diff. peak and hole	0.170 and -0.218 e.Å ⁻³

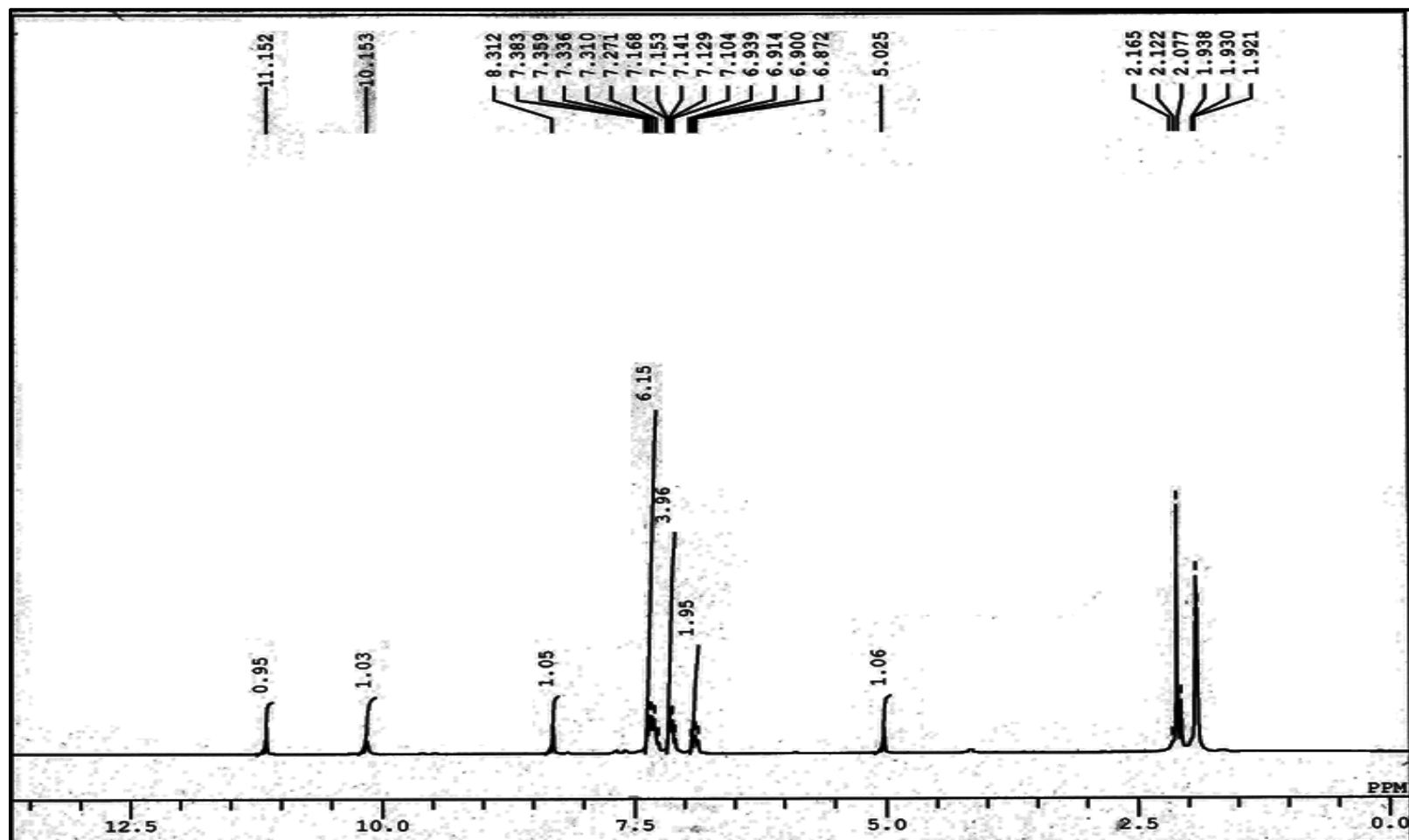
Electronic Supplementary Information

Figure S1: IR spectrum of B-XAN



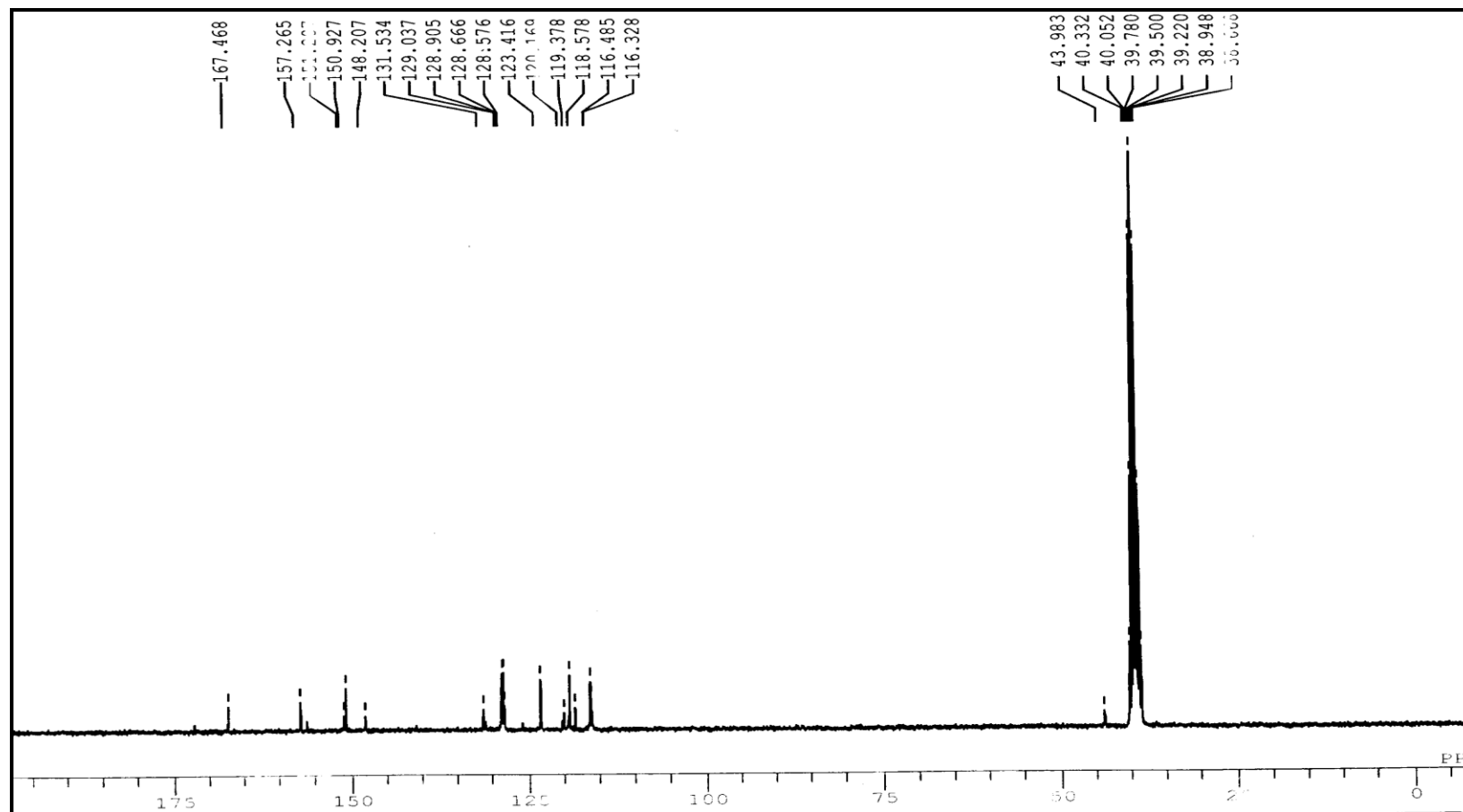
Electronic Supplementary Information

Figure S2: ^1H NMR spectrum of **B-XAN** (in CD_3CN)



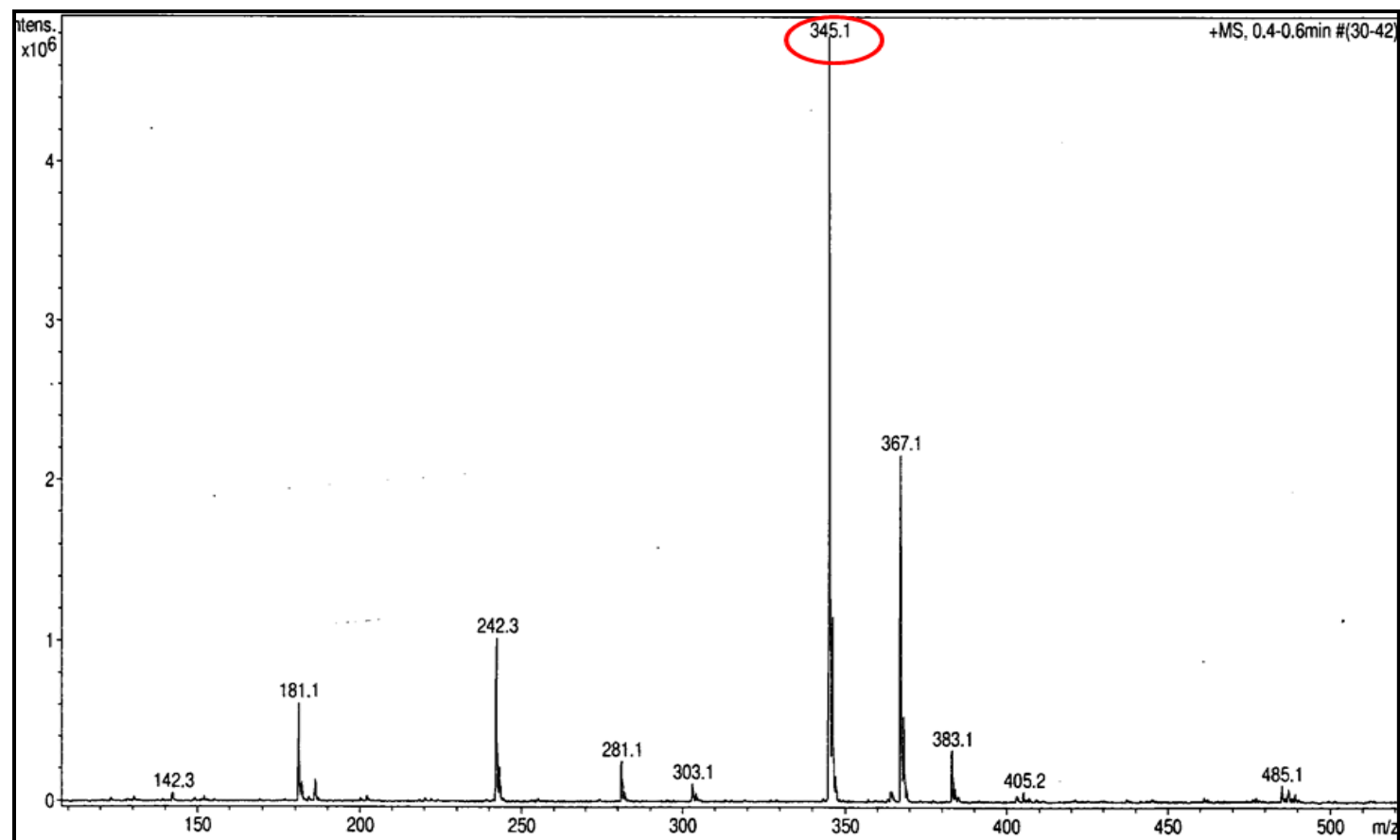
Electronic Supplementary Information

Figure S3: ^{13}C NMR spectrum of **B-XAN** (in $\text{DMSO-}d_6$)



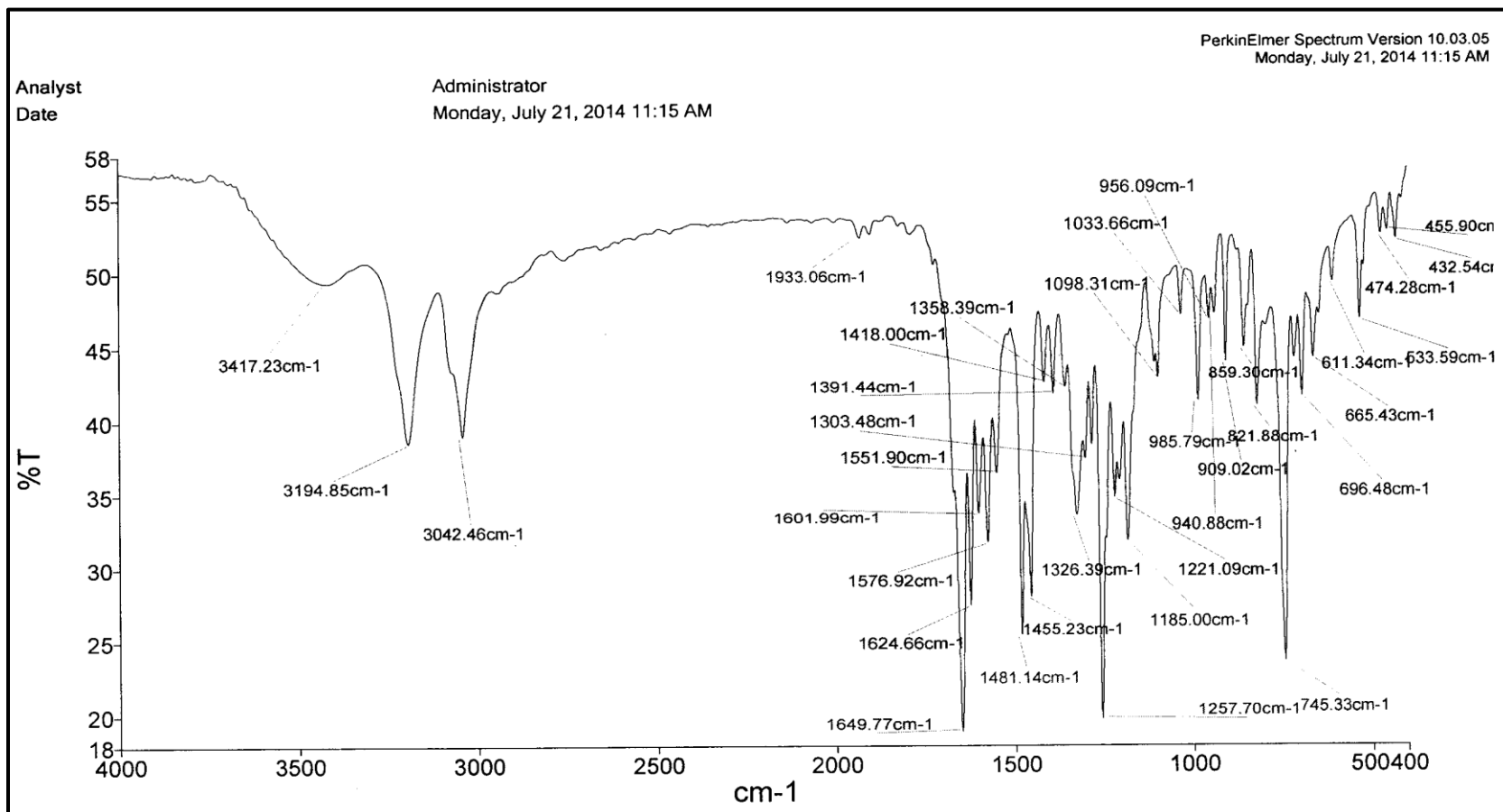
Electronic Supplementary Information

Figure S4: ESI-MS spectrum of B-XAN



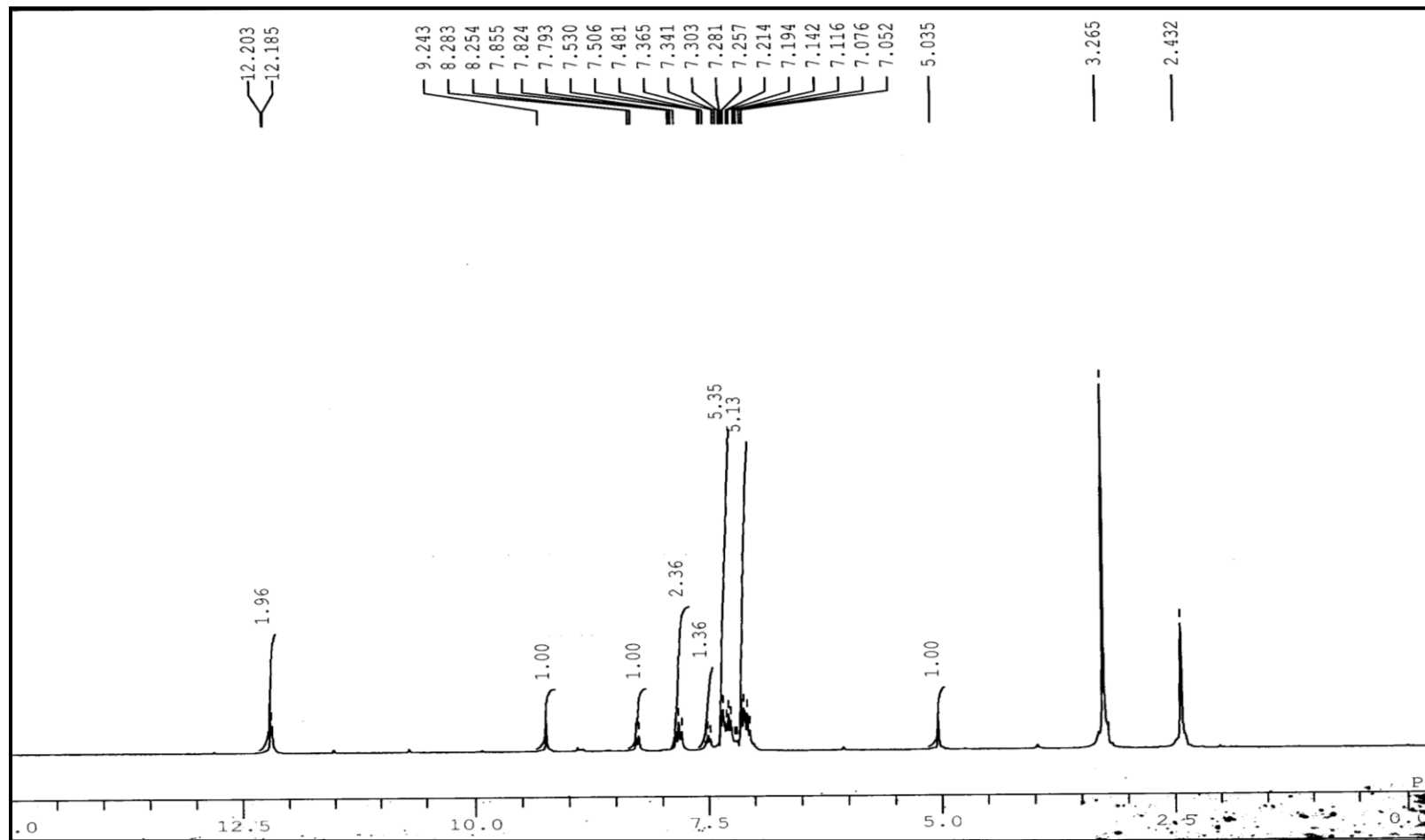
Electronic Supplementary Information

Figure S5: IR spectrum of N-XAN



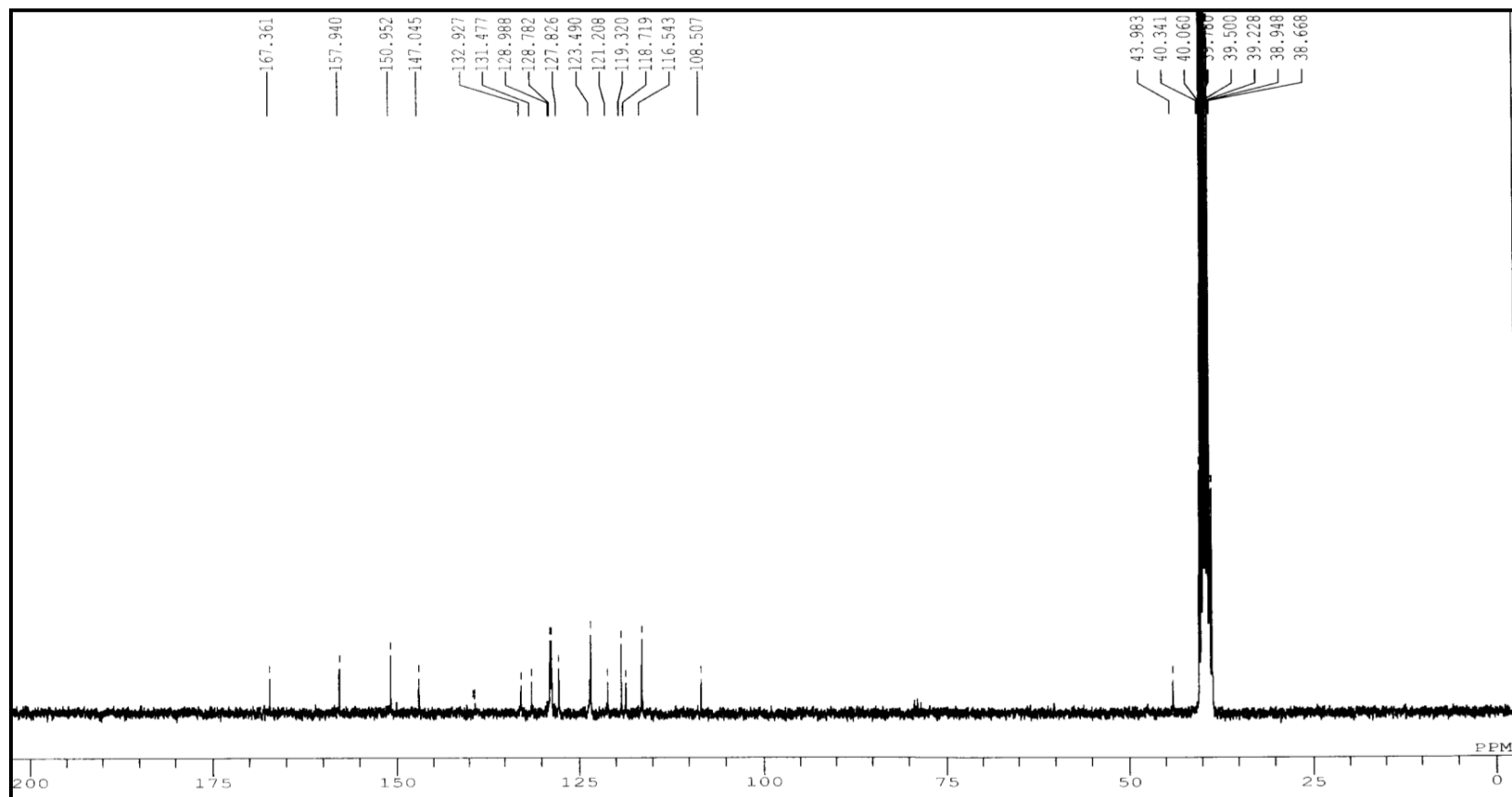
Electronic Supplementary Information

Figure S6: ^1H NMR spectrum of N-XAN (in $\text{DMSO}-d_6$)



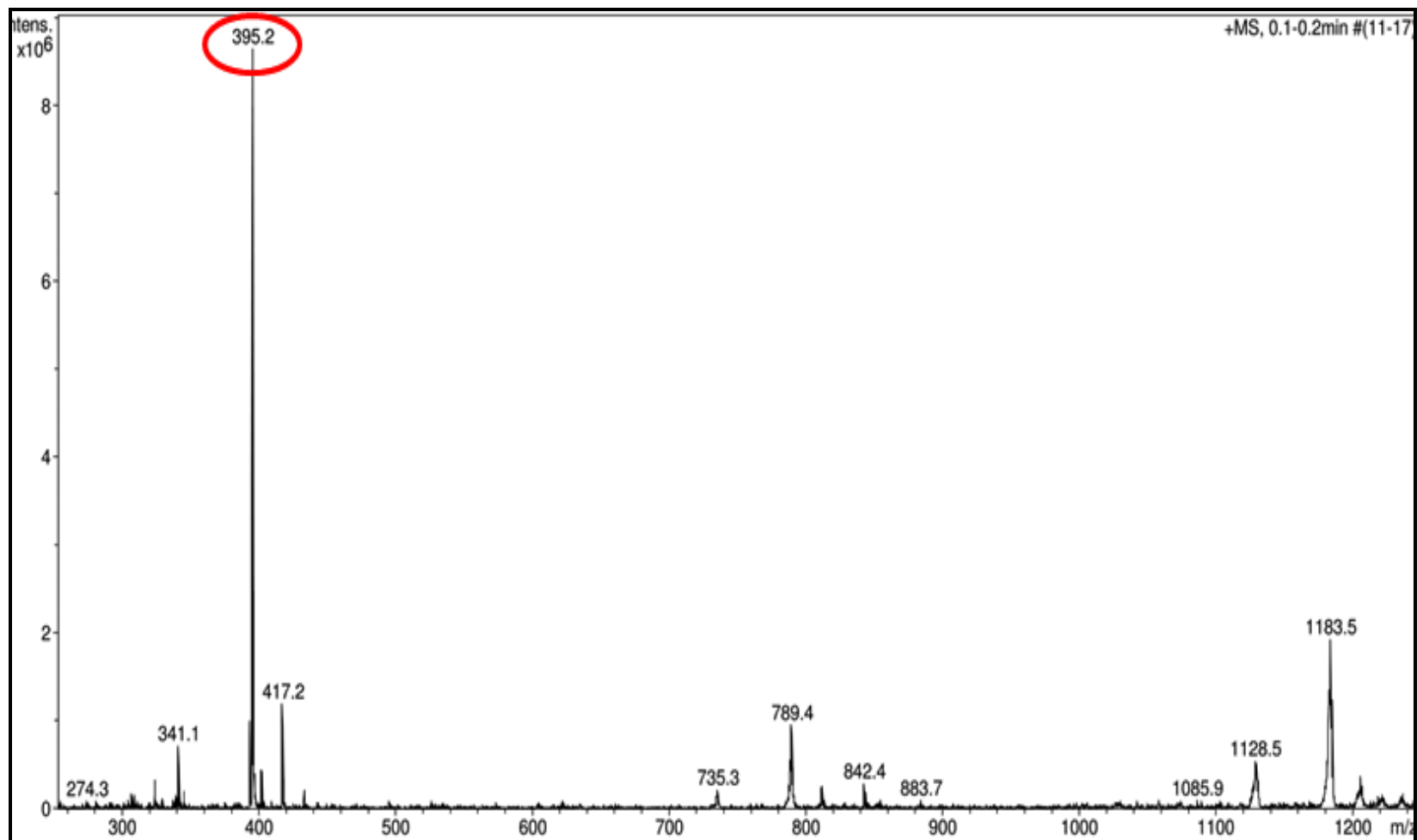
Electronic Supplementary Information

Figure S7: ^{13}C NMR spectrum of N-XAN (in $\text{DMSO-}d_6$)



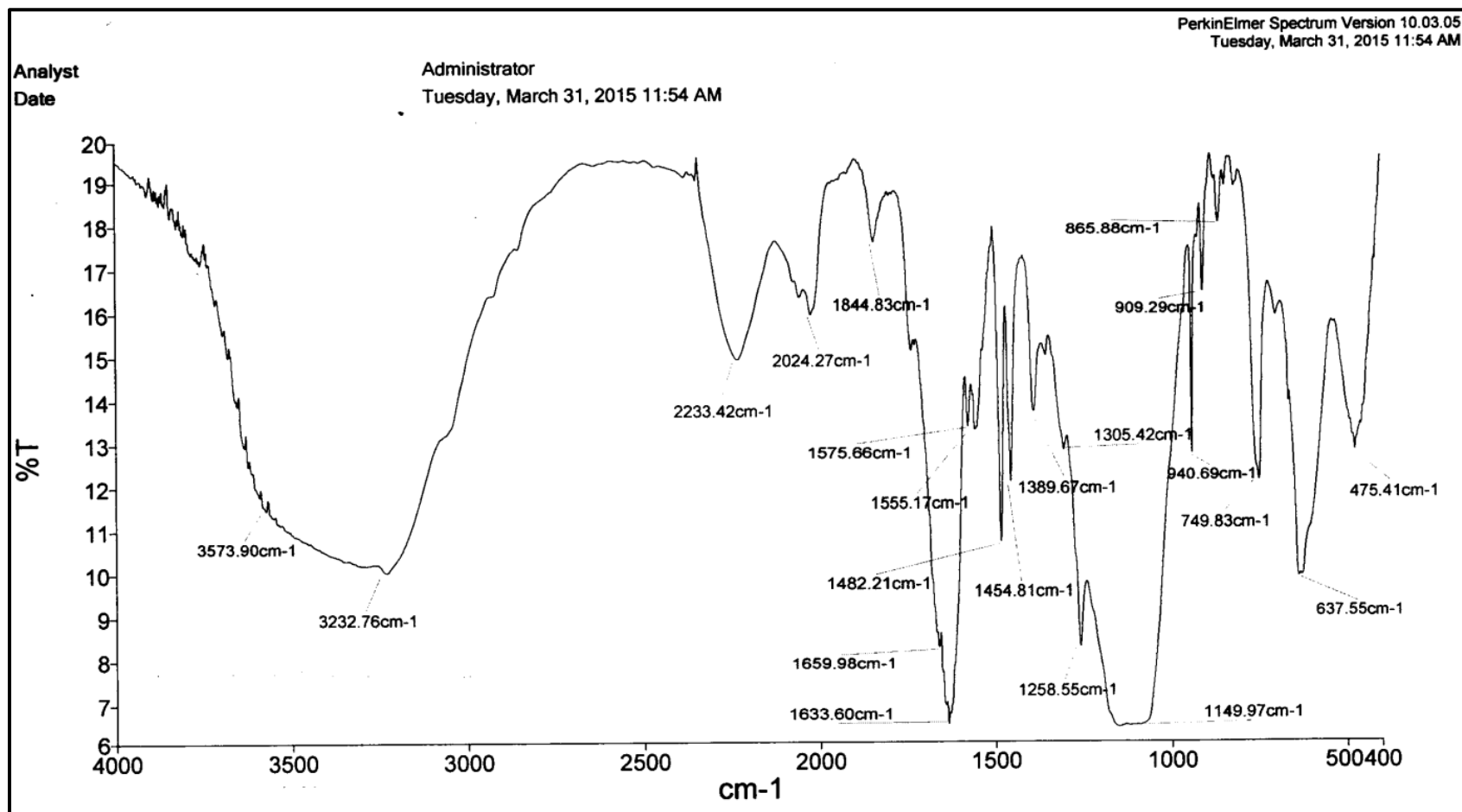
Electronic Supplementary Information

Figure S8: ESI-MS spectrum of N-XAN



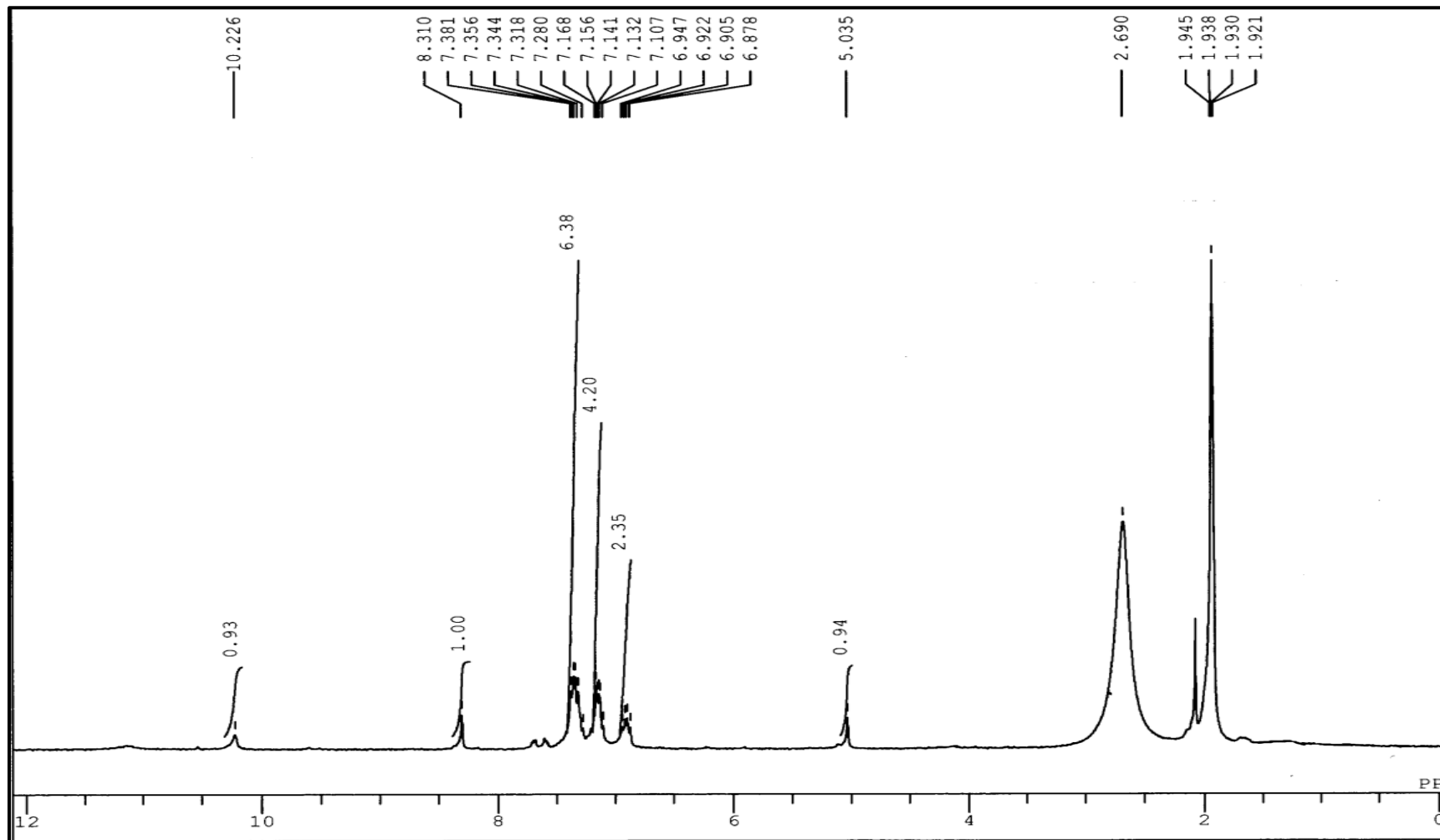
Electronic Supplementary Information

Figure S9: IR spectrum of (B-XAN)₂Mg



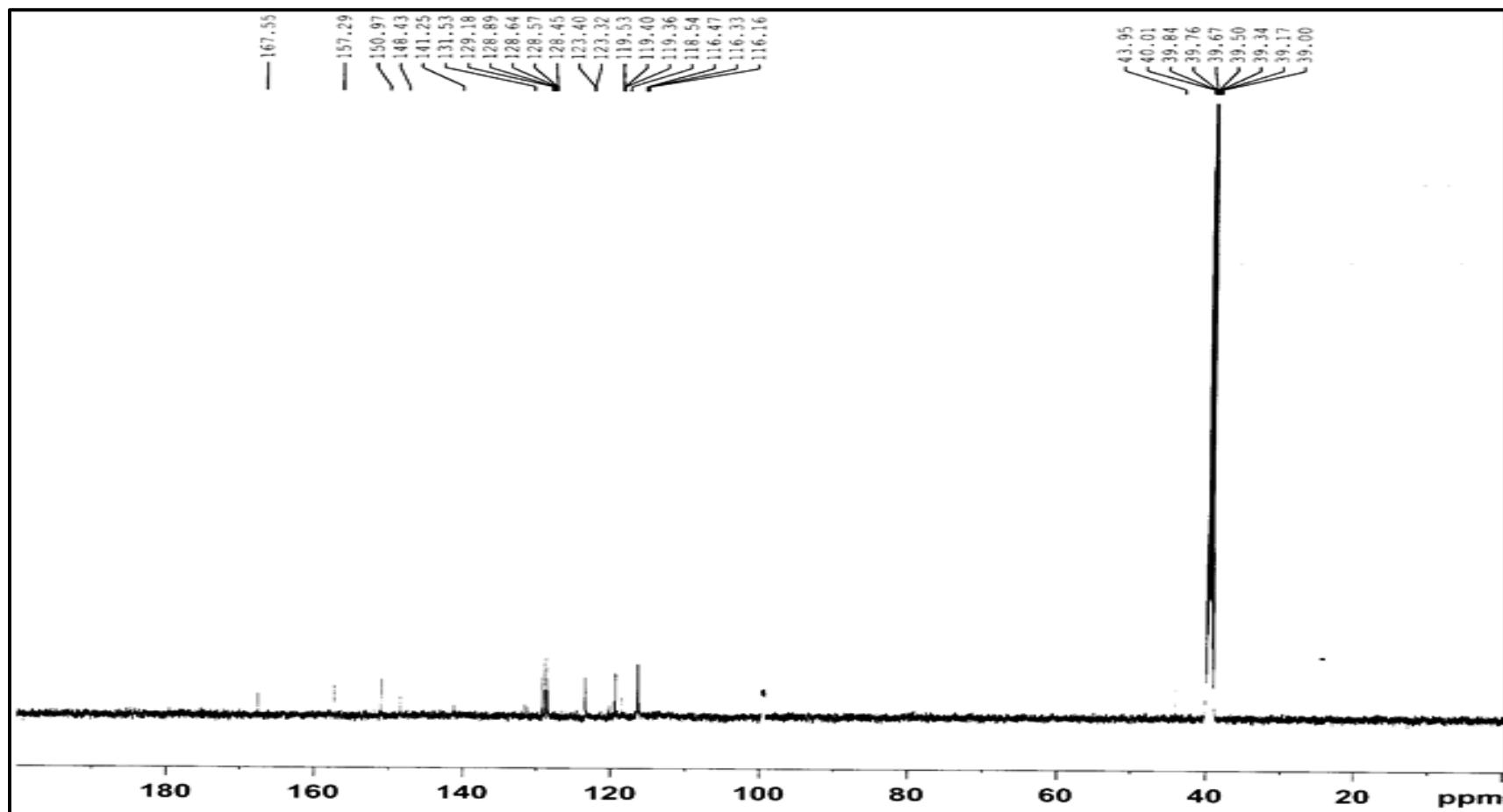
Electronic Supplementary Information

Figure S10: ^1H NMR spectrum of $(\text{B-XAN})_2\text{Mg}$ (in CD_3CN)



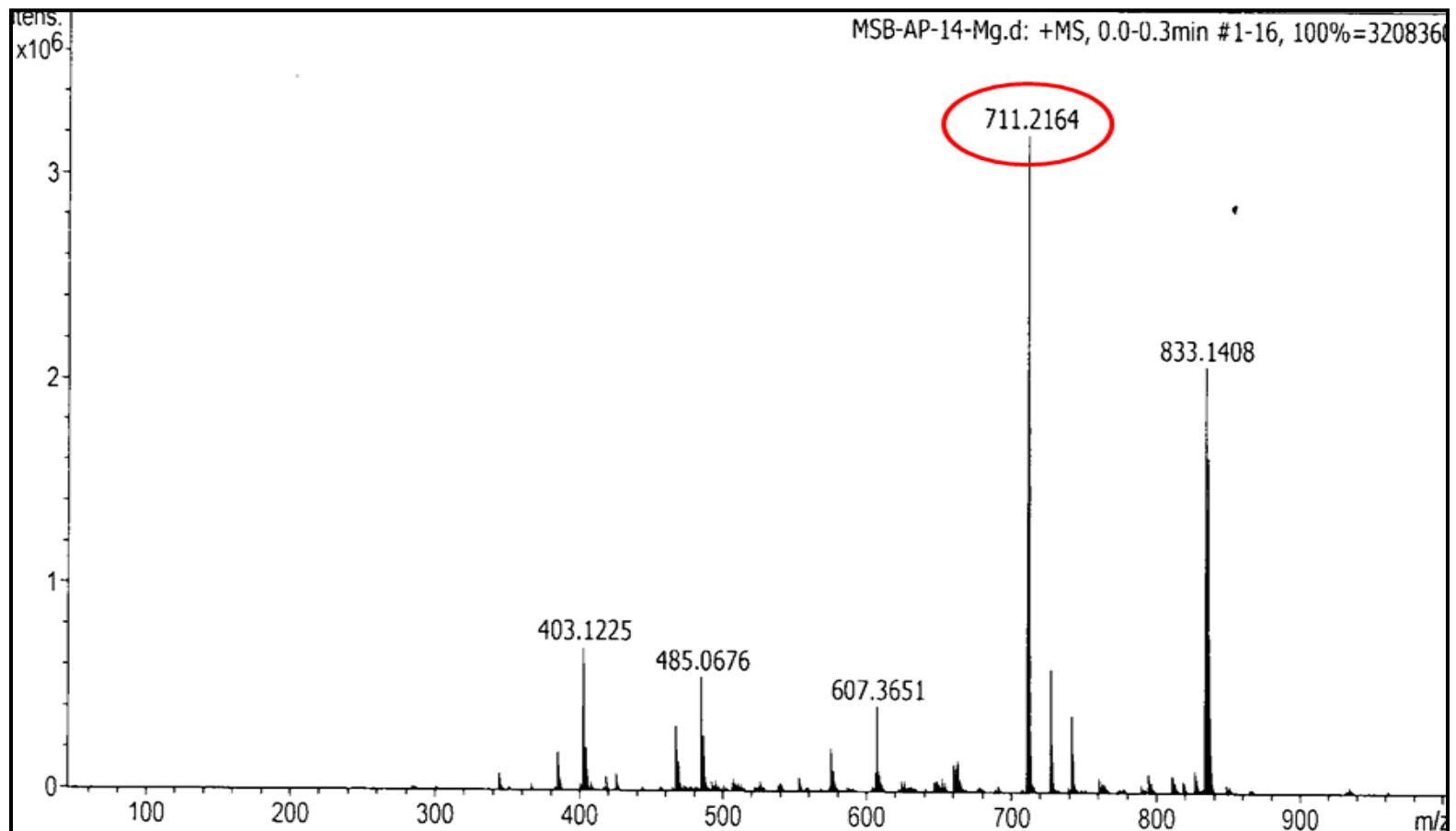
Electronic Supplementary Information

Figure S11: ^{13}C NMR spectrum of $(\text{B-XAN})_2\text{Mg}$ (in $\text{DMSO-}d_6$)



Electronic Supplementary Information

Figure S12: Mass spectrum of (B-XAN)₂Mg



Electronic Supplementary Information

Figure S13 (a): UV-visible spectrum of **B-XAN** with different metal ions (10 equiv.) at 10 μM in acetonitrile

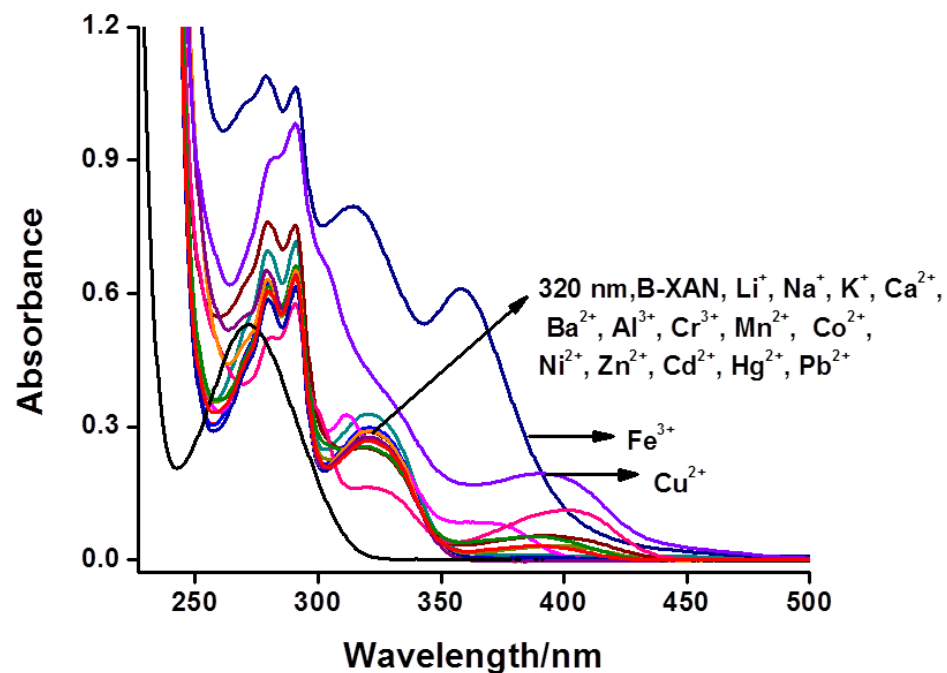


Figure S13 (b): Photograph showing naked eye color change of **B-XAN** (under visible light) in presence of different metal ions in acetonitrile



Electronic Supplementary Information

Figure S14 (a): UV-visible spectrum of N-XAN with different metal ions (10 equiv.) at 10 μM in acetonitrile

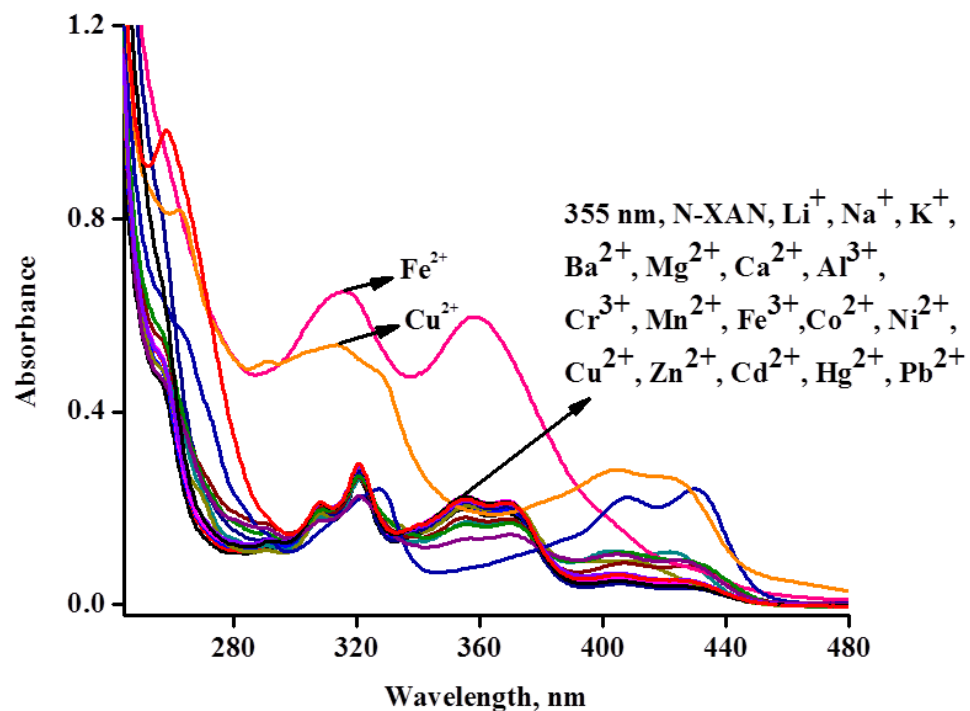
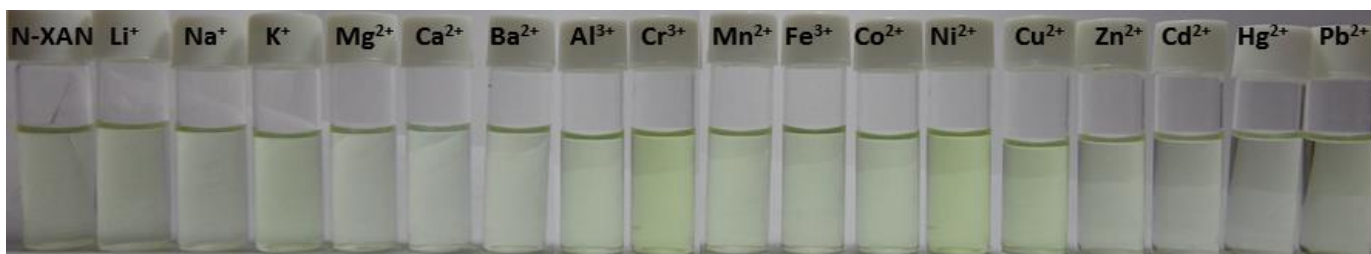


Figure S14 (b): Photograph showing naked eye colour change of N-XAN (under visible light) in presence of different metal ions in acetonitrile



Electronic Supplementary Information

Figure S15 (a): Relative fluorescence changes of N-XAN (1.0 μM) after addition of 10 equiv. of various metal ions in acetonitrile at 458 nm along with inset fluorescence spectral graph.

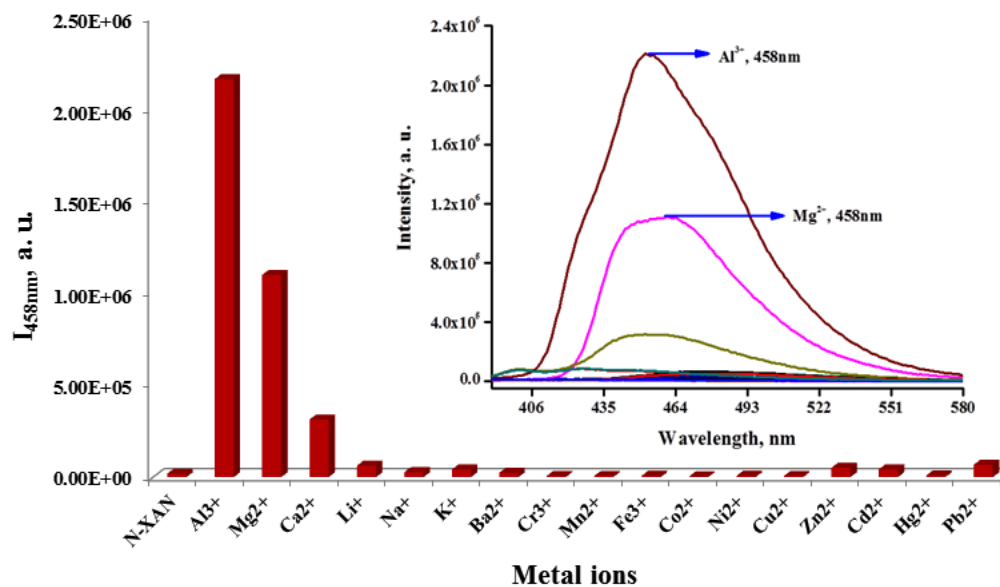
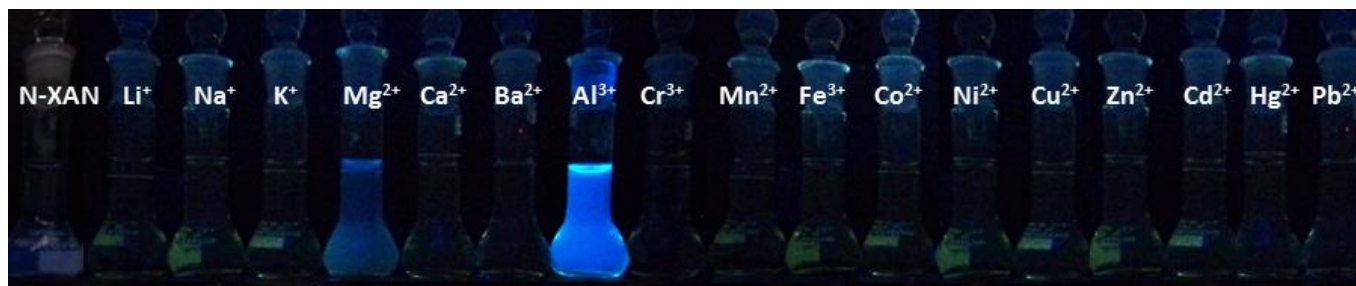
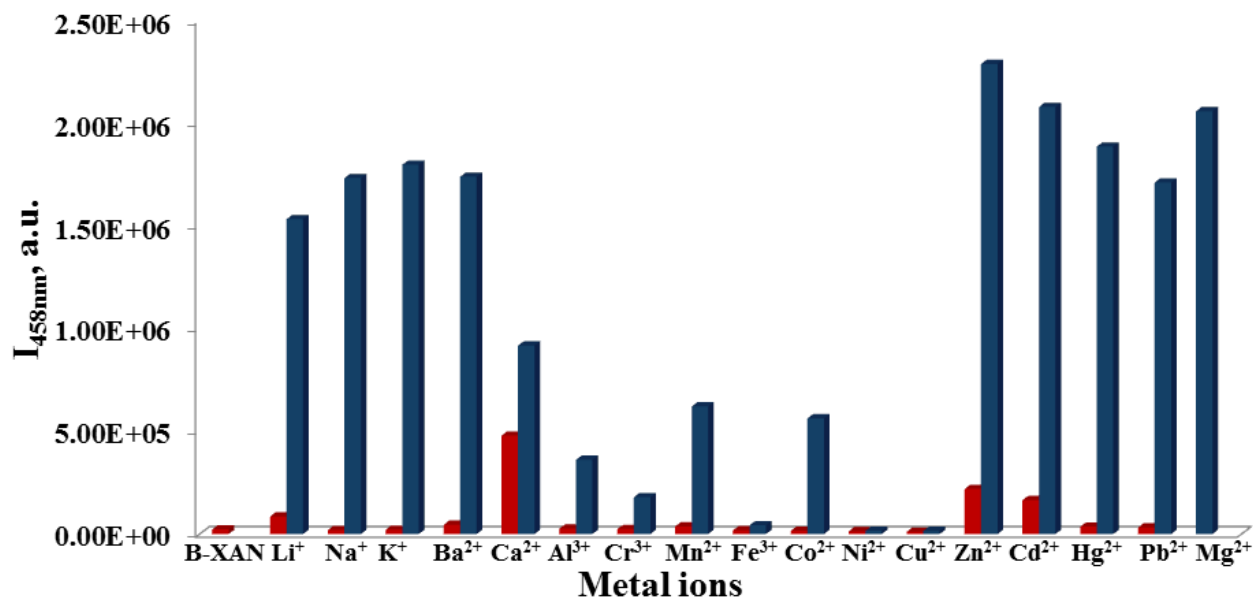


Figure S15 (b): Naked eye fluorescence response of N-XAN in the presence of different metal ions (under UV light of 365 nm)



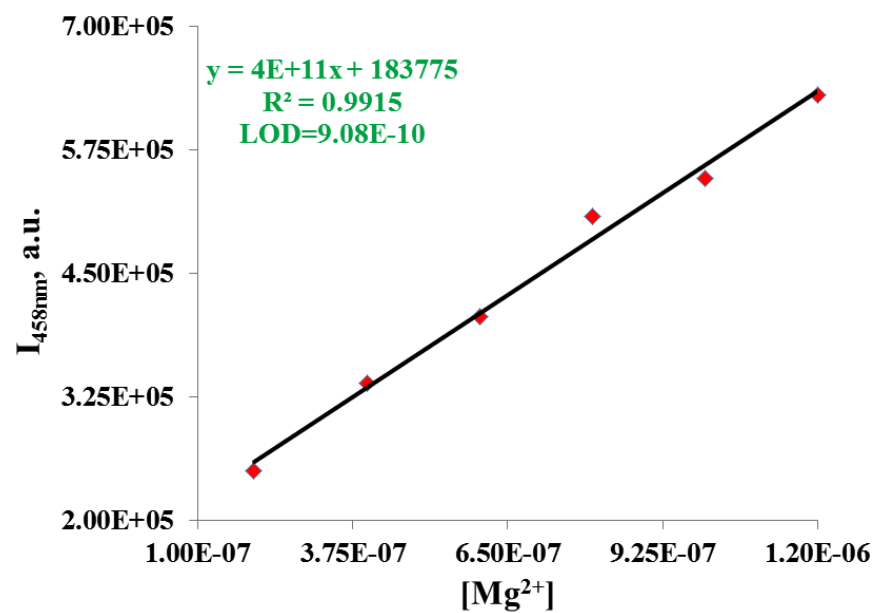
Electronic Supplementary Information

Figure S16: Fluorescence responses of **B-XAN** ($1\mu\text{M}$) at $\lambda_{\text{ex}}=458\text{ nm}$ in the presence of various cations in acetonitrile solution. The red bars represent the emission intensities of **B-XAN** in the presence of various cations (10.0 eq.). The blue bars represent the change of emission upon subsequent addition of Mg^{2+} (10.0 eq.) to the above solution.



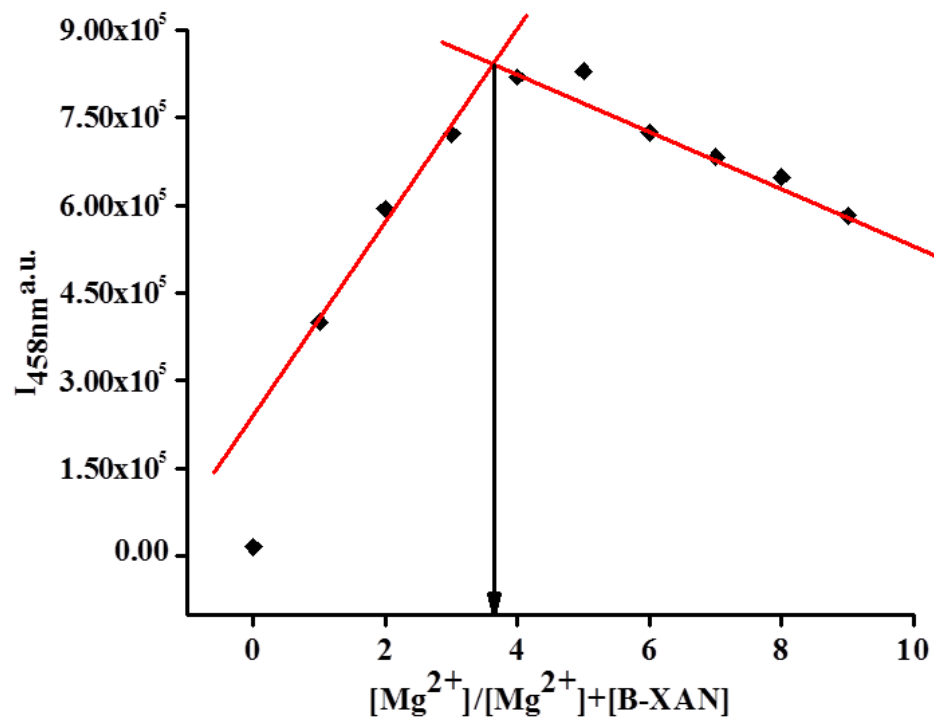
Electronic Supplementary Information

Figure S17: Calibration curve for determination of detection limit of **B-XAN** for Mg^{2+} by fluorescence titration data



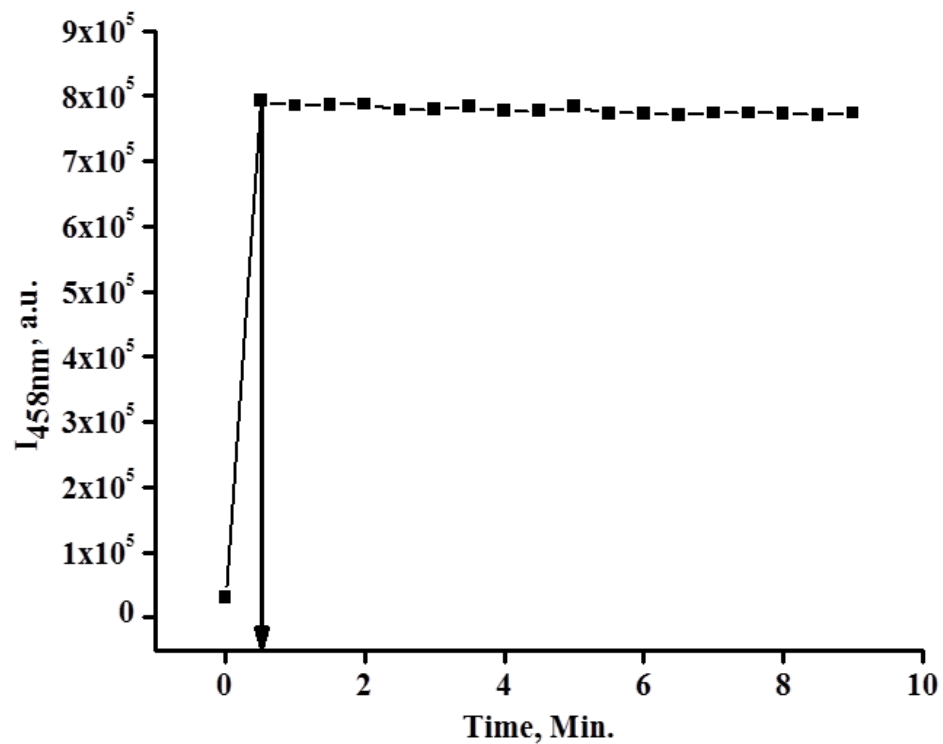
Electronic Supplementary Information

Figure S18: Job's Plot between B-XAN and Mg^{2+} showing 2:1 binding stoichiometry



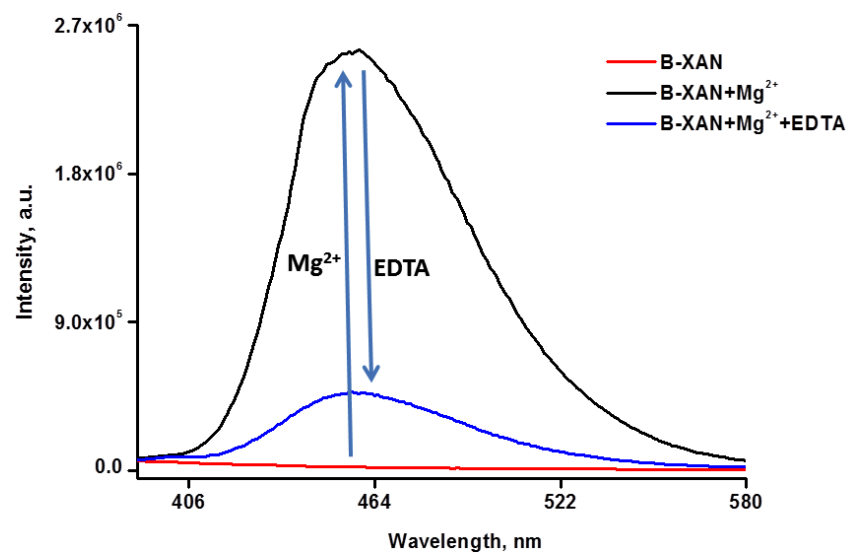
Electronic Supplementary Information

Figure S19: Reaction-time profile of **B-XAN** in presence of Mg^{2+}



Electronic Supplementary Information

Figure S20: Fluorescence emission spectra showing reversibility of **B-XAN** in the presence of Mg^{2+} and EDTA in acetonitrile solution



Electronic Supplementary Information

Figure S21: Non-linear fit plot of fluorescence titration data for determination of binding constants

